Amrit Suman et al. 2023, 11:4
ISSN (Online): 2348-4098
ISSN (Print): 2395-4752

International Journal of Science, Engineering and Technology

An Open Access Journal

CFD Analysis Of Enhancement Of Solar Air Heater Using W-Shaped Roughness

M.Tech. Scholar Amrit Suman, Prof. Brijendra Kumar Yadav
Department of Mechanical Engineering, PCST Bhopal

Abstract- Fossil fuel reservoirs are finite, making the current trajectory of energy consumption and growth unsustainable in the long term. To address this, harnessing solar energy efficiently emerges as a promising solution. Among renewable sources, solar energy stands out, with the conversion of solar radiation into thermal energy proving to be a simple and effective method for various applications like space heating, agricultural product drying, and industrial processes, facilitated by solar air heaters. However, the efficiency of these heaters is hampered by a low convective heat transfer coefficient between the absorber plate and the passing air, mainly due to the presence of a viscous sub-layer. In this study CFD analysis of solar air heater has been done.

Keywords- Solar air heater, w-shaped roughness, heat transfer, thermo eletric air duct.

I. INTRODUCTION

Solar air heaters boast a straightforward design and construction, finding applications in space heating and crop drying as effective solar energy collection devices. However, the efficiency of flat plate solar air heaters remains modest due to the low convective heat transfer coefficient between the absorber plate and the flowing air, leading to elevated absorber plate temperatures and increased heat losses to the surroundings. The presence of a laminar sub-layer is responsible for the low heat transfer coefficient, and this can be mitigated by introducing artificial roughness on the heat-transferring surface [1]

Efforts to enhance heat transfer have revolved around disrupting or destabilizing this laminar sub-layer. Introducing artificial roughness, often in the form of ribs and various configurations, serves to induce turbulence near the wall or break the laminar sub-layer. However, such modifications result in heightened frictional losses, necessitating greater power for fluid flow. Therefore, turbulence generation should be focused on the immediate vicinity of the heat-transferring surface to disrupt the viscous sub-layer, while minimizing disturbances to the core fluid flow to limit additional pumping requirements. Achieving this balance involves ensuring that the dimensions of the roughness elements remain small compared to the duct dimensions [2]. Solar energy emerges as a highly valuable renewable resource, offering substantial benefits for the environment. Its applications span electricity generation, heating, and various industrial processes. Solar air heaters (SAHs) stand as uncomplicated yet efficient solar thermal collectors [1]. These cost-effective devices form a vital part of solar energy utilization systems [2].

Figure 1 illustrates the different components of a solar air heater. These heaters absorb sunlight and convert it into thermal energy on the absorber surface, subsequently transferring the heat to a fluid flowing through the collector. The absorber plate, usually a thin metal sheet coated with an absorbing substance like black or selective coating, captures solar radiation. The glazing provides a sturdy, protective structure for the entire collector assembly, while insulation beneath the absorber and fluid passages minimizes downward heat loss. SAHs find use in numerous solar energy applications, particularly in space heating, wood drying, and agricultural processes[3].

II. RESEARCH METHODOLOGY

1.Computational domain

© 2023 Amrit Suman et al. This is an Open Access article distributed under the terms of the Creative Commons Attribution License (http://creativecommons.org/licenses/by/4.0), which permits unrestricted use, distribution, and reproduction in any medium, provided the original work is properly credited.

A rectangular section was considered.The domain on which numerical simulations were performed was three-dimensional. Their rectangular duct was of length 1500 mm, width 200 mm and thickness 25 mm.Fig. 1 shows the geometry of the computational domain.The rib roughness can be defined by the continuous rib with angle of attack is $90^{o.}$ Simulation using CFD has been done by varying Re number from 2000-to 10000.Constant heat flux of value approximately 1000 W/m^2 was supplied only on the upper wall of the absorber plate. Simulations were performed assuming the flow to be steady.

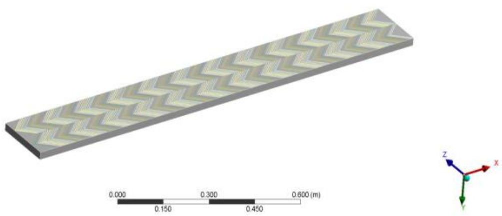

Fig. 1: Computational domain for CFD

Table 1: Operating and Geometrical parameters used for CFD analysis

Operating and Geometrical parameters	Value / Range
Length of duct	1500 mm
Width of duct	200 mm
Thickness of duct	25 mm
Constant heat flux	1000 W/m^2
Range of Reynolds number	2300-18000
Height of rib	0.8 mm
Attack angle	60°

2.Governing differential equations

Continuity equation

$$\frac{\partial}{\partial x_i}(\rho u_i)=0$$

(3.1)

Momentum Equation

$$\frac{\partial}{\partial x_i}(\rho u_i u_j)=-\frac{\partial P}{\partial x_i}+\frac{\partial}{\partial x_j}\left[\mu\left(\frac{\partial u_i}{\partial x_j}+\frac{\partial u_j}{\partial x_i}\right)\right]+\frac{\partial}{\partial x_j}\left(-\rho\overline{u_i'u_j'}\right)$$

(3.2)

Energy equation

$$\frac{\partial}{\partial x_i}(\rho u_i T)=\frac{\partial}{\partial x_j}\left[(\Gamma+\Gamma_t)\frac{\partial T}{\partial x_j}\right]$$

(3.3)

3.Boundary Condition

The rectangular duct's walls, including the roughened surface, were all subjected to no-slip boundary conditions. A consistent heat flux of 1000 W/m² was maintained as the boundary condition on the upper wall of the absorber plate. The inlet was characterized by uniform velocity and an inlet temperature of 300 K, while the exit was governed by constant pressure conditions (atmospheric pressure). The remaining edges were designated as walls with insulation-based boundary conditions.

4.CFD Modelling

Commercially available ANSYS FLUENT v 15.0 was the CFD software employed to solve the concerned general differential equations numerically. This software numerically simulates using finite element method.

III. RESULTS AND DISCUSSION

1.Estimation of heat transfer coefficient at different Reynolds number

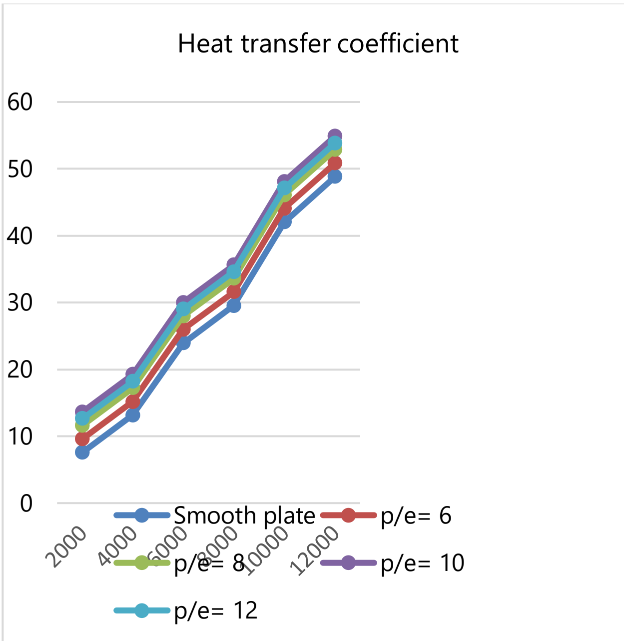

Fig.2: Estimation of heat transfer coefficient at different Reynolds number

Fig. 2show the effect of heat transfer coefficient on Reynolds number. The horizontal x-axis represents Reynolds number and y-axis represents heat transfer coefficient. Heat transfer coefficient increases with an increase of Reynolds number asexpected due to change in fluid flow characteristics as result of roughness which causes flow separation, reattachment and generation of secondary flows.

2.Effect of Pitch to Rib- Height Ratio on Nusselt Number

Effect of relative roughness height on Nusselt number is shown in Fig3. The horizontal x-axis represents pitch-to-height ratio and y-axis represents Nusselt number. It is seen thatincrease in pitch-to-height ratio results in increase in Nusselt number and it is maximum at p/e=10. Thismay be due to the fact that at higher values of relative roughnessheight, reattachment of free shear layer might not occur and rate ofheat transfer enhancement is not proportional to that of frictionfactor.

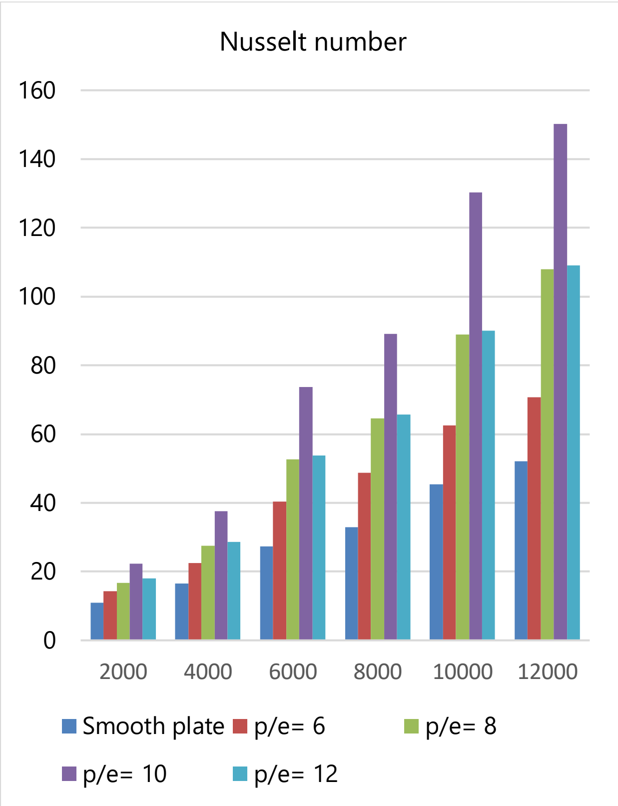

Fig.3: Variation of Nusselt at different pitch to rib-height ratio

3.Effect of Pitch to Rib- Height Ratio on Friction Factor

Effect of relative roughness height on friction factor is shown in Fig. 4.The horizontal x-axis represents pitch-to-height ratio and y-axis represents friction factor. It is seen thatincrease in pitch-to-height ratio results in increase in friction factor and it is maximum at p/e=10. Thismay be due to the fact that at higher values of relative roughnessheight, reattachment of free shear layer might not occur and rate ofheat transfer enhancement is not proportional to that of friction factor.

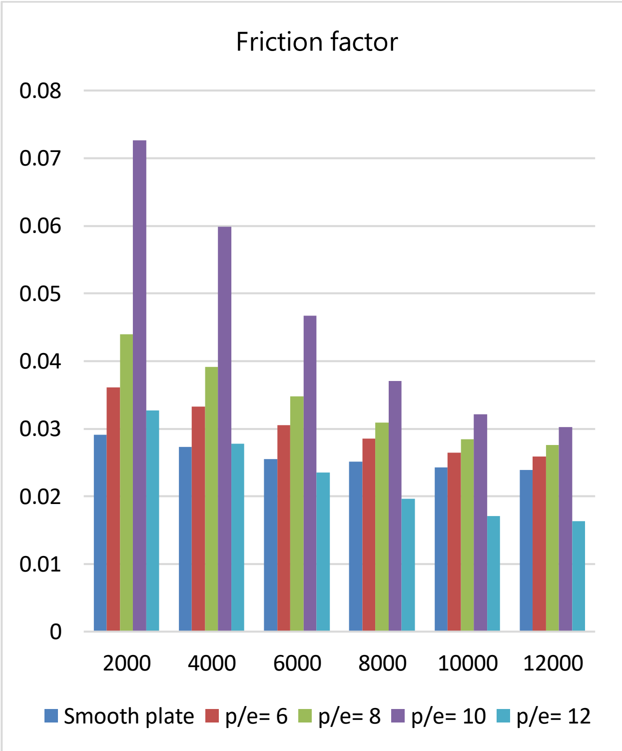

Fig. 4 Variation of friction factor at different pitch to rib- height ratio

IV. CONCLUSION

As the Reynolds number increases, the Nusselt number shows an upward trend while the friction factor experiences a decline. Comparatively higher values of friction factor and Nusselt number are noted in contrast to those observed for a smooth absorber plate. This phenomenon arises from the altered flow characteristics attributed to surface roughness, causing flow separation, subsequent reattachment, and generation of secondary flow.

The rate of Nusselt number augmentation with escalating Reynolds number is less pronounced than the rate of friction factor increases. This discrepancy arises primarily from conditions where higher relative roughness height inhibits the reattachment of the free shear layer. Consequently, the enhancement in heat transfer does not scale proportionally to the increase in friction factor.

The peak enhancement in both Nusselt number and friction factor occurs at a pitch-to-height ratio (p/e) of 10. This optimized value is a result of the interplay between flow separation, secondary flow generation induced by W-shaped ribs, and the motion of vortices, leading to an ideal angle of attack.

1. Across all cases explored in this study, an increase in Reynolds number corresponds to an augmentation in Nusselt number.
2. Introduction of ribs or baffles directly beneath the collector plate induces a substantial alteration in the heat transfer coefficient of the air.

REFERENCES

1. Agrawal, Y., Yugbodh, K., Ahmed, S. F., Jain, E., Bhagoria, J. L., Gautam, A., & Mishra, A. (2023). Experimental investigation of heat transfer and flow analysis of artificially roughened solar air heater by using double arc reverse shaped roughness with gap on the absorber plate. Materials Today: Proceedings, 78, 403-413.
2. Fadala, G. M., & Yousef, A. H. (2023). The effect of artificial roughness on performance of solar air heater (SAH): A review study. In AIP Conference Proceedings (Vol. 2776, No. 1, p. 050008). AIP Publishing LLC.
3. Chaurasia, S., Goel, V., &Debbarma, A. (2023). Impact of hybrid roughness geometry on heat transfer augmentation in solar air heater: A review. Solar Energy.
4. Saxena, R., Pachorkar, P., Jain, A., Majumder, H., Pandey, K. K., Mishra, S. K., &Kalbande, V. P. (2023). Performance enhancement of solar air heater using artificial roughness. Materials Today: Proceedings.
5. Yadav, A. K., Choudhary, M., & Singh, A. P. (2023). Assessment of solar air heater performance using a variety of artificially roughened components. Materials Today: Proceedings.
6. Singh, V. P., Jain, S., & Gupta, J. M. L. (2023). Analysis of the effect of perforation in multi-v rib artificial roughened single pass solar air heater:-Part A. Experimental Heat Transfer, 36(2), 163-182.
7. Kumar, D., &Layek, A. (2023). Heat Transfer Enhancement of Solar Air Heater Having Twisted V-Shaped Staggered Roughness Over Absorber Plate. Arabian Journal for Science and Engineering, 48(3), 3931-3946.
8. Arya, N., Goel, V., &Sunden, B. (2023). Solar air heater performance enhancement with differently shaped miniature combined with dimple shaped roughness: CFD and experimental analysis. Solar Energy, 250, 33-50.
9. Kumar, D., &Layek, A. (2022). Parametric analysis of artificial rib roughness for the enhancement of thermohydraulic performance of solar air heater: A review. Materials Today: Proceedings, 57, 1127-1135.
10. Singh, H., Singh, H., & Kishore, C. (2022). CFD numerical investigation of Heat transfer characteristics of Y-shaped solar air heater. Materials Today: Proceedings, 52, 2003-2013.
11. Yadav, A. S., Gupta, S., Agrawal, A., Saxena, R., Agrawal, N., &Nashine, S. (2022). Performance enhancement of solar air heater by attaching artificial rib roughness on the absorber Plate. Materials Today: Proceedings, 63, 706-717.
12. Bhuvad, S. S., Azad, R., &Lanjewar, A. (2022). Thermal performance analysis of apex-up discrete arc ribs solar air heater-an experimental study. Renewable Energy, 185, 403-415.
13. Agrawal, Y., Bhagoria, J. L., Gautam, A., Sharma, A., Yadav, A. S., Alam, T., & Kumar, R. (2023). Investigation of thermal performance of a ribbed solar air heater for sustainable built environment. Sustainable Energy Technologies and Assessments, 57, 103288.
14. Alsaiari, A. O., Iqbal, A., Abdulkhair, H., Gzara, L., Almatrafi, E., Alzahrani, H. A., ... &Aljohani, M. (2022). Heat transmission and air flow friction in a solar air heater with a ribbed absorber plate: A computational study. Case Studies in Thermal Engineering, 40, 102517.
15. Agrawal, Y., &Bhagoria, J. L. (2021). Experimental investigation for pitch and angle of arc effect of discrete artificial roughness on Nusselt number and fluid flow characteristics of a solar air heater. Materials Today: Proceedings, 46, 5506-5511.
16. Azad, R., Bhuvad, S., &Lanjewar, A. (2021). Study of solar air heater with discrete arc ribs geometry: Experimental and numerical approach. International Journal of Thermal Sciences, 167, 107013.

17. Patel, S. S., &Lanjewar, A. (2021). Experimental investigation of solar air heater duct with discrete V-rib integrated with staggered elements. International Journal of Sustainable Engineering, 14(2), 162-171.
18. Kumar, P. G., Balaji, K., Sakthivadivel, D., Vigneswaran, V. S., Velraj, R., & Kim, S. C. (2021). Enhancement of heat transfer in a combined solar air heating and water heater system. Energy, 221, 119805.